

Nonhyperbolic reflection moveout for horizontal transverse isotropy

AbdulFattah Al-Dajani* and Ilya Tsvankin†

ABSTRACT

The transversely isotropic model with a horizontal axis of symmetry (HTI) has been extensively used in studies of shear-wave splitting to describe fractured formations with a single system of parallel vertical penny-shaped cracks. Here, we present an analytic description of long-spread reflection moveout in horizontally-layered HTI media with arbitrary strength of anisotropy.

The hyperbolic moveout equation parameterized by the exact normal-moveout (NMO) velocity is sufficiently accurate for P -waves on conventional-length spreads (close to the reflector depth), although the NMO velocity is not, in general, usable for converting time to depth. However, the influence of anisotropy leads to the deviation of the moveout curve from a hyperbola with increasing spreadlength, even in a single-layer model. To account for nonhyperbolic moveout, we have derived an exact expression for the azimuthally-dependent quartic term of the Taylor series travelttime expansion $[t^2(x^2)]$ valid for any pure mode in an HTI layer. The quartic moveout coefficient and the normal-moveout velocity are then substituted into the nonhyperbolic moveout equation of Tsvankin and Thomsen, originally designed for vertical

*Formerly Center for Wave Phenomena, Colorado School of Mines, Golden, CO 80401; presently Earth Resources Laboratory, Massachusetts Institute of Technology, Cambridge, MA 02142-1324. E-mail: dajani@erl.mit.edu

†Department of Geophysics, Colorado School of Mines, Golden, CO 80401.

transverse isotropy (VTI media). Numerical examples for media with both moderate and uncommonly strong nonhyperbolic moveout show that this equation accurately describes azimuthally-dependent P -wave reflection traveltimes in an HTI layer, even for spreadlengths twice as large as the reflector depth.

In multilayered HTI media, the NMO velocity and the quartic moveout coefficient reflect the influence of layering, as well as azimuthal anisotropy. We show that the conventional Dix equation for NMO velocity remains entirely valid for any azimuth in HTI media if the *group-velocity* vectors (rays), for data in a common-midpoint (CMP) gather, do not deviate from the vertical incidence plane. Although this condition is not exactly satisfied in the presence of azimuthal velocity variations, rms averaging of the interval NMO velocities represents a good approximation for models with moderate azimuthal anisotropy. Furthermore, the quartic moveout coefficient for multilayered HTI media can also be calculated with acceptable accuracy using the known averaging equations for vertical transverse isotropy. This allows us to extend the nonhyperbolic moveout equation to horizontally stratified media composed of any combination of isotropic, VTI, and HTI layers. In addition to providing analytic insight into the behavior of nonhyperbolic moveout, these results can be used in modeling and inversion of reflection traveltimes in azimuthally anisotropic media.

INTRODUCTION

Recent field studies (Lynn et al., 1996; Corrigan et al., 1996) have shown that P -wave reflection moveout and amplitude-variation-with-offset (AVO) response may be strongly influenced by the presence of azimuthal anisotropy. However, the current understanding of seismic signatures in general azimuthally anisotropic media is hardly sufficient for the inversion and processing of seismic data, even if the medium is horizontally homogeneous. This work is devoted to an analytic description of long-spread reflection moveout in the transversely isotropic model with a horizontal axis of sym-

metry (HTI media) – the simplest type of azimuthally anisotropic media associated with a system of parallel vertical penny-shaped cracks embedded in an isotropic matrix (Crampin, 1985; Thomsen, 1988). Weak-anisotropy approximations for reflection moveout in HTI media were discussed by Thomsen (1988), Sena (1991) and Li and Crampin (1993); the latter paper also treats reflection traveltimes in an orthorhombic layer. Sayers and Ebrom (1997) extended Sena’s (1991) nonhyperbolic moveout equation to an orthorhombic or monoclinic layer with a horizontal symmetry plane. However, since the approach of Sayers and Ebrom (1997) is based on the expansion of group velocity into spherical harmonics, their moveout coefficients are difficult to relate to the medium parameters. Also, the moveout equations of Sena (1991) and Sayers and Ebrom (1997) contain the reflector depth – a quantity usually unknown in reflection surveys, which makes their formalism more suitable for VSP applications.

An exact equation for azimuthally-dependent normal-moveout velocity for pure modes in a single HTI layer was presented by Tsvankin (1997). He also showed that all kinematic signatures including normal moveout (as well as plane-wave polarizations) in the symmetry plane of HTI media that contains the symmetry axis (“the symmetry-axis” plane) are given by equations of the same form as for transversely isotropic media with a *vertical* symmetry axis (VTI). The analogy between HTI and VTI media allowed Tsvankin (1997) and Rüger (1997) to introduce Thomsen’s (1986) parameters for HTI media using exactly the same expressions as for vertical transverse isotropy. This notation proved to be much more convenient in describing reflection signatures than the generic Thomsen coefficients defined with respect to the symmetry axis. For instance, the *P*-wave NMO velocity in HTI media depends on the vertical velocity, azimuth of the symmetry axis, and a single anisotropic coefficient – the parameter $\delta^{(V)}$ expressed through the stiffnesses in the same way as is Thomsen’s coefficient δ for VTI media (Tsvankin, 1997).

Despite these developments, some important issues pertaining to moveout analysis for horizontal transverse isotropy remained unresolved. Among them is the analytic

description of long-spread (nonhyperbolic) moveout in HTI media and the feasibility of obtaining interval NMO velocities in the presence of pronounced azimuthal anisotropy and vertical inhomogeneity. Both problems have to be examined *outside* the vertical symmetry planes of HTI media, since reflection moveout within the symmetry planes is identical to that in VTI media.

It is well known that reflection moveout in anisotropic media is generally nonhyperbolic, unless the anisotropy is elliptical. Hake et al. (1984) derived the quartic Taylor series term A_4 of $t^2 - x^2$ reflection-moveout curves for pure modes in TI media with a vertical axis of symmetry. Tsvankin and Thomsen (1994) obtained the coefficient A_4 for converted $P - SV$ waves and represented the quartic terms of the pure modes in a more compact form using Thomsen's (1986) notation. They also developed a nonhyperbolic moveout equation for layered VTI media, based on the exact quadratic (NMO velocity) and quartic moveout coefficients, that converges at infinitely large horizontal offsets as well. In TI media with a vertical symmetry axis, this equation remains close to the exact P -wave moveout for spreads as large as three times the reflector depth. The moveout expression of Tsvankin and Thomsen (1994) will serve as a basis for our study of nonhyperbolic reflection moveout in HTI media.

Nonhyperbolic moveout can hamper the estimation of normal-moveout velocity using conventional hyperbolic semblance analysis (e.g., Gidlow and Fatti, 1990). Tsvankin (1997) gives a numerical example showing that in a single HTI layer the hyperbolic moveout equation parameterized by the exact NMO velocity remains accurate up to the spreadlength equal to the reflector depth. In layered media, however, the magnitude of nonhyperbolic moveout may increase due to vertical velocity variations and deviations of group-velocity vectors (rays) of reflected waves from the incidence plane. Even if the analytic normal-moveout velocity for a stack of layers has been extracted from finite-spread moveout, it is not clear whether *interval* NMO velocities can be obtained from the Dix equation, which is no longer strictly valid outside the symmetry planes of azimuthally anisotropic media.

In this paper, we derive a concise expression for the quartic moveout coefficient valid for all pure modes in a homogeneous HTI layer with anisotropy of any strength. The quadratic and quartic moveout coefficients in multilayered HTI media are obtained by the same averaging equations as for vertical transverse isotropy. These results are used to extend the nonhyperbolic equation of Tsvankin and Thomsen (1994) to horizontal transverse isotropy. Numerical testing demonstrates high accuracy of our nonhyperbolic moveout equation, even for media with significant depth-varying azimuthal anisotropy and pronounced nonhyperbolic moveout.

DESCRIPTION OF THE HTI MODEL AND NOTATION

In this section, we describe the main features of the HTI model and a convenient Thomsen-style notation for horizontal transverse isotropy introduced by Tsvankin (1997) and Rüger (1997). Proper understanding of wave propagation in the two mutually orthogonal vertical symmetry planes (Figure 1) is extremely important in the analysis of seismic signatures in HTI media. In the plane normal to the symmetry axis (the isotropy plane), body-wave velocities are independent of direction, and the influence of anisotropy manifests itself only through the different velocities of the two S -waves (The split shear waves in HTI media will be denoted as “ S^{\parallel} ” and “ S^{\perp} ”, with the S^{\parallel} -wave polarized within the isotropy plane and the S^{\perp} -wave polarized in the plane formed by the symmetry axis and the slowness vector.). In the second vertical symmetry plane, which contains the axis of symmetry (the “symmetry-axis plane”), the velocities do change with propagation angle, but the Christoffel equation has exactly the same form as in transversely isotropic media with a *vertical* symmetry axis. This means that the phase velocity and polarization vector are the same functions of the stiffness coefficients and phase angle with vertical as in VTI media. Since phase velocity determines group (ray) velocity and group angle, all kinematic signatures in the symmetry-axis plane, including normal-moveout velocity and long-spread

(nonhyperbolic) reflection moveout, are given by the known VTI equations.

Taking advantage of this limited equivalence, Tsvankin (1997) and Rüger (1997) introduced the Thomsen parameters of the “equivalent” VTI model through the same equations as those used by Thomsen (1986) for actual VTI media. For the HTI model with the symmetry axis in the x_1 -direction, the stiffness coefficients c_{ij} and density ρ , these parameters are defined as

$$\begin{aligned}
 V_{P_{vert}} &\equiv \sqrt{\frac{c_{33}}{\rho}}, \\
 V_{S^{\perp}_{vert}} &\equiv \sqrt{\frac{c_{55}}{\rho}}, \\
 \epsilon^{(V)} &\equiv \frac{c_{11} - c_{33}}{2c_{33}}, \\
 \delta^{(V)} &\equiv \frac{(c_{13} + c_{55})^2 - (c_{33} - c_{55})^2}{2c_{33}(c_{33} - c_{55})}, \\
 \gamma^{(V)} &\equiv \frac{c_{66} - c_{44}}{2c_{44}},
 \end{aligned} \tag{1}$$

where $V_{P_{vert}}$ and $V_{S^{\perp}_{vert}}$ are the vertical velocities of the P - and S^{\perp} -wave, respectively (note that in our HTI model $c_{55} = c_{66}$). The vertical velocity of the (fast) shear wave S^{\parallel} is determined as

$$V_{S^{\parallel}_{vert}} \equiv \sqrt{\frac{c_{44}}{\rho}} = \frac{V_{S^{\perp}_{vert}}}{\sqrt{1 + 2\gamma^{(V)}}}.$$

This notation makes it possible to obtain the kinematic signatures and polarizations in the symmetry-axis plane of HTI media just by adapting the corresponding equations for vertical transverse isotropy expressed through Thomsen parameters. The convenient features of Thomsen notation in the analytic description of seismic wavefields in VTI media were summarized by Tsvankin (1996). Furthermore, as discussed in more detail below, the Thomsen coefficients of the equivalent VTI model control the moveout *outside* the symmetry planes of HTI media, where the analogy with VTI media is no longer valid.

The exact expressions for the phase velocity in HTI media in terms of the parameters $\epsilon^{(V)}$, $\delta^{(V)}$, and $\gamma^{(V)}$ were presented in Tsvankin (1997). For P - and S^{\perp} -waves,

the phase velocity is given by

$$\frac{V^2(\theta)}{V_{P_{vert}}^2} = 1 + \epsilon^{(V)} \cos^2 \theta - \frac{f^{(V)}}{2} \pm \frac{f^{(V)}}{2} \sqrt{\left(1 + \frac{2\epsilon^{(V)} \cos^2 \theta}{f^{(V)}}\right)^2 - \frac{2(\epsilon^{(V)} - \delta^{(V)}) \sin^2 2\theta}{f^{(V)}}}, \quad (2)$$

where the plus sign corresponds to the P -wave, and the minus to the S^\perp -wave; $f^{(V)} = 1 - (V_{S^\perp_{vert}}/V_{P_{vert}})^2$; and θ is the phase angle with the horizontal symmetry axis. For P -waves, phase velocity and all other kinematic signatures in HTI media depend largely on the vertical velocity $V_{P_{vert}}$ and the coefficients $\epsilon^{(V)}$ and $\delta^{(V)}$, while the influence of the S^\perp -wave vertical velocity (and, therefore, $f^{(V)}$) is practically negligible (Tsvankin, 1997).

Alternatively, HTI media can be characterized by the “generic” Thomsen parameters defined with respect to the symmetry axis. However, since the symmetry axis is horizontal, these parameters (especially the coefficient δ) are not well-suited to describe reflection seismic signatures, which are largely dependent on *near-vertical* velocity variations. The relationships between the two sets of Thomsen parameters can be found in Tsvankin (1997).

Note that the values of the parameters $\epsilon^{(V)}$, $\delta^{(V)}$, and $\gamma^{(V)}$ are quite different from those typical for actual VTI media. While the coefficients ϵ and γ for vertical transverse isotropy are usually non-negative, in HTI media due to thin parallel cracks $\epsilon^{(V)} \leq 0$ and $\gamma^{(V)} \leq 0$. Also, for typical ratios of the vertical velocities ($V_{S^\perp_{vert}}/V_{P_{vert}} \leq 0.707$), the parameter $\delta^{(V)} \leq 0$, which is possible but not typical for such VTI formations as shales. Similar to VTI media, however, the difference $\epsilon^{(V)} - \delta^{(V)}$ that characterizes the “anellipticity” of the medium is typically positive for horizontal transverse isotropy.

ANALYTIC APPROXIMATIONS OF REFLECTION MOVEOUT

Reflection moveout in CMP gathers is conventionally approximated by the hyperbolic equation

$$t^2 = t_0^2 + \frac{x^2}{V_{\text{nmo}}^2}, \quad (3)$$

where t is the reflection travelttime at source-receiver offset x , t_0 is the two-way zero-offset travelttime, and V_{nmo} is the normal-moveout velocity defined in the zero-spread limit.

Equation (3) is strictly valid only for a homogeneous isotropic (or elliptically anisotropic) layer. The presence of layering and/or anisotropy leads to deviation of the travelttime curve from the hyperbola (3) with increasing offset, and the finite-spread moveout (stacking) velocity, usually obtained from hyperbolic semblance analysis, no longer coincides with the analytic NMO velocity. However, for vertical transverse isotropy the hyperbolic moveout equation for P -waves usually provides sufficient accuracy on conventional-length spreads (i.e., spreadlength close to the reflector depth – see Tsvankin and Thomsen, 1994).

Nonhyperbolic moveout on longer spreads can be described by a three-term Taylor series expansion (Taner and Koehler, 1969),

$$t^2 = t_0^2 + A_2x^2 + A_4x^4, \quad (4)$$

where $A_2 = 1/V_{\text{nmo}}^2$, and A_4 is the quartic moveout coefficient. The parameter A_4 for pure modes in horizontally layered VTI media was given by Hake et al. (1984) and represented in a more compact form by Tsvankin and Thomsen (1994).

Due to the influence of the x^4 term, the quartic equation (4) becomes divergent with increasing offset and can be replaced by a more accurate nonhyperbolic moveout equation developed by Tsvankin and Thomsen (1994),

$$t^2 = t_0^2 + A_2x^2 + \frac{A_4x^4}{1 + Ax^2}, \quad (5)$$

where $A = A_4/(1/V_{\text{hor}}^2 - 1/V_{\text{nm0}}^2)$, and V_{hor} is the horizontal velocity. The denominator of the nonhyperbolic term ensures the convergence of this approximation at infinitely large horizontal offsets. As a result, equation (5) provides an accurate description of P -wave traveltimes on long CMP spreads (2-3 times as large as the reflector depth), even for models with pronounced nonhyperbolic moveout.

Although equation (5) was originally designed for vertical transverse isotropy, it could be used in *arbitrary* anisotropic media if the appropriate coefficients A_2 , A_4 , and A were found. Our goal is to extend this nonhyperbolic moveout approximation to single- and multi-layered HTI media. As discussed in the previous section, for a CMP line parallel to the symmetry axis no generalization is necessary, since the moveout in the symmetry-axis plane can be obtained directly from the original VTI equation (5) by substituting the Thomsen coefficients of the equivalent VTI model. Clearly, in the isotropy plane long-spread reflection moveout of any given mode is not influenced by the anisotropy at all. The analogy with VTI media also holds for throughgoing vertical symmetry planes of multilayered models containing VTI and HTI layers.

For CMP lines outside the vertical symmetry planes of HTI media, however, it is necessary to obtain the azimuthally-dependent parameters of equation (5). Below, we accomplish this task for horizontally layered HTI media with arbitrary strength of anisotropy.

MOVEOUT IN A SINGLE HTI LAYER

Normal-moveout and horizontal velocity

The exact P -wave normal-moveout velocity on a CMP line that makes the angle α with the symmetry axis (Figure 2) is given by (Tsvankin, 1997)

$$V_{\text{nm0}}^2(\alpha) = V_{\text{Pvert}}^2 \frac{1 + 2\delta^{(\text{V})}}{1 + 2\delta^{(\text{V})} \sin^2 \alpha}. \quad (6)$$

To obtain the corresponding expressions for the shear waves, $V_{P_{vert}}$ in equation (6) should be replaced with the appropriate vertical velocity, while $\delta^{(V)}$ should be replaced with either $\gamma^{(V)}$ (for the S^{\parallel} -wave) or $\sigma^{(V)} = (V_{P_{vert}}/V_{S_{vert}^{\perp}})^2(\epsilon^{(V)} - \delta^{(V)})$ (for the S^{\perp} -wave); for details, see Tsvankin (1997).

It should be mentioned that the azimuthal dependence of normal-moveout velocity for any pure mode is described by an *elliptical* curve in the horizontal plane. Indeed, equation (6) can be rewritten as

$$V_{\text{nmo}}^2(\alpha) = \frac{V_{\text{nmo}}^2(0) V_{\text{nmo}}^2(90)}{V_{\text{nmo}}^2(0) \sin^2 \alpha + V_{\text{nmo}}^2(90) \cos^2 \alpha},$$

where $V_{\text{nmo}}(0)$ and $V_{\text{nmo}}(90)$ are the NMO velocities in the symmetry-axis and isotropy planes, respectively. Evidently, the axes of the NMO ellipse are aligned with the vertical symmetry planes of the HTI model. This fact may be useful in the detection of the dominant fracture orientation in HTI media. As shown by Grechka and Tsvankin (1996), the azimuthal dependence of NMO velocity remains elliptical even in inhomogeneous, arbitrary anisotropic media.

To obtain the quantity A in the nonhyperbolic moveout equation (5), we also have to find the azimuthally-dependent horizontal group velocity (V_{hor}), which controls reflection moveout at offsets approaching infinity. Since the influence of small errors in V_{hor} can be ignored for spreadlengths feasible in reflection surveys, we will calculate V_{hor} as the phase (rather than the group) velocity evaluated in the azimuth of the CMP line. Therefore, for the P - and S^{\perp} -waves we find the horizontal velocity by substituting $\theta = \alpha$ into equation (2). For S^{\parallel} -waves, as we will demonstrate next, the nonhyperbolic moveout term vanishes, and computing the horizontal velocity is not necessary.

Quartic moveout coefficient

Application of the nonhyperbolic moveout equation (5) also requires knowledge of the quartic moveout coefficient A_4 . An exact expression for A_4 in a single HTI layer

is derived in Appendix A:

$$A_4(\alpha) = \left[-\frac{\frac{4}{V} \frac{d^2V}{d\theta^2} + 3\left(\frac{1}{V} \frac{d^2V}{d\theta^2}\right)^2 + \frac{1}{V} \frac{d^4V}{d\theta^4}}{12t_0^2 V_{vert}^4 \left(1 + \frac{1}{V} \frac{d^2V}{d\theta^2}\right)^4} \right]_{\theta=90^\circ} \cos^4 \alpha = A_4(\alpha = 0) \cos^4 \alpha. \quad (7)$$

As before, α is the angle between the CMP line and the symmetry axis. Equation (7) is valid for HTI models with arbitrary strength of anisotropy and can be used for any pure-mode reflection (P , S^\perp , S^\parallel). The most interesting feature of equation (7) is the simplicity of the azimuthal dependence of the quartic moveout coefficient. The maximum absolute value of A_4 corresponds to the symmetry-axis plane ($\alpha = 0^\circ$), while in the isotropy plane $A_4(\alpha = 90^\circ) = 0$, so moveout is purely hyperbolic. The form of the angular dependence ($\cos^4 \alpha$) implies that the quartic coefficient rapidly decreases with azimuth away from the symmetry-axis plane.

The term $A_4(\alpha = 0)$ represents the quartic coefficient in the symmetry-axis plane, where all moveout parameters are given by the same equations as for vertical transverse isotropy. Although an equivalent expression was obtained by Hake et al. (1984), here $A_4(\alpha = 0)$ is represented for the first time as a simple function of phase velocity and its derivatives. In addition to the axis orientation, the influence of anisotropy on the quartic moveout coefficient is absorbed by just two velocity terms: $\frac{1}{V} \frac{d^2V}{d\theta^2} \Big|_{\theta=90^\circ}$ and $\frac{1}{V} \frac{d^4V}{d\theta^4} \Big|_{\theta=90^\circ}$.

To find the quartic coefficient for the P -wave, we evaluate the second and fourth derivatives of phase velocity using equation (2):

$$\frac{1}{V} \frac{d^2V}{d\theta^2} \Big|_{\theta=90^\circ} = 2\delta^{(V)}, \quad (8)$$

and

$$\frac{1}{V} \frac{d^4V}{d\theta^4} \Big|_{\theta=90^\circ} = 24(\epsilon^{(V)} - \delta^{(V)}) \left(1 + \frac{2\delta^{(V)}}{f^{(V)}}\right) - 2\delta^{(V)}(4 + 6\delta^{(V)}). \quad (9)$$

Substituting equations (8) and (9) into equation (7), we obtain an explicit expression for the P -wave quartic moveout coefficient:

$$A_4^{(P)}(\alpha) = \left[\frac{-2(\epsilon^{(V)} - \delta^{(V)}) \left(1 + \frac{2\delta^{(V)}}{f^{(V)}}\right)}{t_0^2 V_{Pvert}^4 (1 + 2\delta^{(V)})^4} \right] \cos^4 \alpha. \quad (10)$$

As expected from the analogy between the symmetry-axis plane of HTI media and vertical transverse isotropy, the expression in brackets $[A_4(\alpha = 0^\circ)]$ in equation (10) is identical to the P -wave quartic coefficient for VTI media given in Tsvankin and Thomsen (1994). Alkhalifah and Tsvankin (1995) showed that the contribution of the shear-wave vertical velocity to the P -wave quartic coefficient in VTI media can be ignored without degrading the quality of the nonhyperbolic moveout equation. Then P -wave nonhyperbolic moveout for vertical transverse isotropy becomes a function of just two effective parameters: the normal-moveout velocity V_{nmo} and the anisotropic coefficient $\eta \equiv (\epsilon - \delta)/(1 + 2\delta)$. This conclusion remains entirely valid for the P -wave quartic moveout coefficient in HTI media, with V_{nmo} and η calculated in the symmetry-axis plane. Indeed, setting the shear-wave vertical velocity in equation (10) to zero ($f^{(V)} = 1$) yields a two-parameter representation of $A_4^{(P)}(\alpha)$:

$$A_4^{(P)}(\alpha) \approx \left[\frac{-2\eta^{(V)}}{t_0^2 V_{\text{nmo}}^4} \right] \cos^4 \alpha, \quad (11)$$

where $V_{\text{nmo}} = V_{\text{nmo}}(\alpha = 0) = V_{P0} \sqrt{1 + 2\delta^{(V)}}$ and $\eta^{(V)} \equiv (\epsilon^{(V)} - \delta^{(V)})/(1 + 2\delta^{(V)})$. Therefore, P -wave NMO velocity, quartic moveout coefficient and nonhyperbolic moveout as a whole are largely controlled by the axis orientation and three parameters – V_{P0} , $\delta^{(V)}$, and $\epsilon^{(V)}$ (or, alternatively, by the two NMO velocities in the symmetry planes and the parameter $\eta^{(V)}$).

Similarly, for the S^\perp -wave, using equation (2) yields

$$\left. \frac{1}{V} \frac{d^2 V}{d\theta^2} \right|_{\theta=90^\circ} = 2\sigma^{(V)},$$

and

$$\left. \frac{1}{V} \frac{d^4 V}{d\theta^4} \right|_{\theta=90^\circ} = -24\sigma^{(V)} \left(1 + \frac{2\delta^{(V)}}{f^{(V)}} \right) - 2\sigma^{(V)} (4 + 6\sigma^{(V)}).$$

Hence, equation (7) takes the form

$$A_4^{(S^\perp)}(\alpha) = \left[\frac{2\sigma^{(V)}(1 + 2\delta^{(V)}/f^{(V)})}{t_0^2 V_{S^\perp \text{vert}}^4 (1 + 2\sigma^{(V)})^4} \right] \cos^4 \alpha. \quad (12)$$

Again, the expression in brackets in equation (12) is identical to the S^\perp -wave quartic coefficient in VTI media given in Tsvankin and Thomsen (1994), which represents a useful check of our results.

For the shear wave S^\parallel , the anisotropy is elliptical, so that $A_4^{(S^\parallel)}(0)$ vanishes. According to equation (7), this means that the quartic moveout term for the S^\parallel -wave vanishes in all other azimuthal directions as well, and S^\parallel -wave moveout in a single HTI layer is purely hyperbolic.

Thus, the last two sections provide the expressions for the NMO velocity, the quartic moveout coefficient, and the horizontal velocity needed to construct the non-hyperbolic moveout equation (5) for a single HTI layer.

MOVEOUT IN MULTILAYERED MEDIA

In multilayered anisotropic media, both the quadratic and quartic moveout coefficients reflect the combined influence of layering as well as anisotropy. On conventional-length spreads, the hyperbolic moveout equation (3) can be expected to provide an adequate description of moveout, but the NMO velocity should be averaged over the stack of layers. For vertical transverse isotropy, this averaging is performed by means of the conventional isotropic Dix (1955) equation (Hake et al., 1984). Furthermore, Alkhalifah and Tsvankin (1995) showed that the Dix equation remains valid in symmetry planes of any anisotropic medium (even if the reflector is dipping), provided the interval NMO velocities are evaluated at the ray-parameter value for the zero-offset ray. In Appendix B we extend the Dix-type equation of Alkhalifah and Tsvankin to arbitrary CMP directions in azimuthally anisotropic media under the assumption that the *group-velocity* vector does not deviate from the vertical incidence plane (the orientation of the phase-velocity vector in this case has no influence on the results). For horizontal interfaces, the ray parameter of the zero-offset ray is always zero, and our generalized NMO equation (B-4) reduces to the

conventional Dix (rms) formula,

$$V_{\text{nmo}}^2 = \frac{1}{t_0} \sum_{i=1}^N V_{\text{nmoi}}^2 \Delta t_i, \quad (13)$$

where t_0 is the two-way zero-offset time to reflector N, V_{nmoi} is the NMO velocity for each individual layer i , and Δt_i is the two-way zero-offset time in layer i . The interval NMO velocity V_{nmoi} for any wave type in HTI media was discussed above.

As shown in Appendix B, rms averaging of the interval velocities remains valid in azimuthally anisotropic media if the group-velocity vector (ray) is confined to the incidence plane for the whole raypath. This assumption is strictly valid in a single HTI layer (as well as in any other homogeneous layer with a horizontal symmetry plane). For off-symmetry azimuthal directions in multilayered HTI media, both group- and phase-velocity vectors may deviate from the incidence plane to satisfy Snell's law at each interface. However, incident and reflected rays usually lie closer to the incidence plane than the corresponding phase vectors because each ray has to return to the CMP line at the receiver location. Deviation of rays from the incidence plane are especially small in stratified models with a similar character of azimuthal velocity variations in all layers (e.g., in HTI media with depth-invariant azimuth of the symmetry axis). Tsvankin et al. (1997) extended the Dix equation to account for arbitrary ray trajectories in azimuthally anisotropic media, but the discussion of this more general expression is outside of the scope of this paper. Here, we will restrict ourselves to implementing equation (13) and studying its accuracy in multilayered HTI models.

To use the nonhyperbolic moveout equation (5) in multilayered media, we also need to incorporate the influence of layering into the quartic moveout term. The exact coefficient A_4 for pure modes in VTI media was presented by Hake et al. (1984):

$$A_4 = \frac{(\sum_{i=1}^N V_{\text{nmoi}}^2 \Delta t_i)^2 - t_0 \sum_{i=1}^N V_{\text{nmoi}}^4 \Delta t_i}{4(\sum_{i=1}^N V_{\text{nmoi}}^2 \Delta t_i)^4} + \frac{t_0 \sum_{i=1}^N A_{4i} V_{\text{nmoi}}^8 \Delta t_i^3}{(\sum_{i=1}^N V_{\text{nmoi}}^2 \Delta t_i)^4}, \quad (14)$$

where A_{4i} is the quartic moveout coefficient for layer i .

The first term in the right-hand side of equation (14) has the same form as for isotropic media (Al-Chalabi, 1974), but it contains the interval NMO velocities which are different from the true vertical velocities in the presence of anisotropy. The second term goes to zero in isotropic or elliptically anisotropic media and, therefore, represents a purely anisotropic contribution to the quartic moveout coefficient. Tsvankin and Thomsen (1994) showed that the nonhyperbolic moveout equation (5) with the quartic term given by equation (14) accurately describes P -wave reflection moveout in multilayered VTI media.

Outside the symmetry planes of stratified HTI media, both phase- and group-velocity vectors deviate from the incidence plane, violating the main assumptions behind the VTI averaging [equation (14)]. Nonetheless, we apply equation (14) to horizontal transverse isotropy, but with the *exact* expressions for the interval values V_{nmoi} [equation (6)] and A_{4i} [equation (7)], which honor the azimuthal dependence of the moveout coefficients. Therefore, in the numerical examples below, both the quadratic and quartic moveout coefficients in layered HTI media are calculated using the same averaging equations as for VTI media, but with the exact interval values derived for horizontal transverse isotropy.

For layered media, the effective horizontal velocity (V_{hor}) contained in the quantity A of the nonhyperbolic moveout equation (5) can be computed in several different ways (Tsvankin and Thomsen, 1994; Alkhalifah, 1997). In theory, V_{hor} should be equal to the maximum horizontal velocity of the medium above the reflector. While this choice of horizontal velocity makes equation (5) converge at infinite source-receiver offsets x , it may generate somewhat inaccurate results at intermediate x feasible for reflection surveys, especially in the presence of thin high-velocity layers (Alkhalifah, 1997). We have found that the highest accuracy for HTI models with typical gradients in the vertical velocity (e.g., 0.5-0.8 s^{-1}) is provided by fourth-power averaging:

$$V_{\text{hor}}^4 = \frac{1}{t_0} \sum_{i=1}^N V_{\text{hor}_i}^4 \Delta t_i, \quad (15)$$

where V_{hor_i} is the interval horizontal velocity in layer i . As discussed above, for purposes of moveout modeling the interval horizontal velocity V_{hor_i} in HTI media can be well approximated by the phase velocity [equation (2)] evaluated at the azimuth of the CMP line.

Another possible alternative is to compute the effective horizontal velocity as the rms average of the interval values of V_{hor} (Tsvankin and Thomsen, 1994). Our numerical tests show that rms averaging works well in HTI media with relatively small gradients in vertical velocity ($\leq 0.3 \text{ s}^{-1}$), but is less suitable for media with more pronounced vertical inhomogeneity. Also, this choice of V_{hor} cannot be used to account for nonhyperbolic moveout in stratified isotropic or elliptically anisotropic media. Indeed, in such media the rms-averaged NMO velocity and horizontal velocity are equal to each other, the coefficient A in the denominator of the nonhyperbolic moveout term goes to infinity, and equation (5) reduces to the hyperbolic equation (3).

The approximations made in this section allow us to apply the concise averaging equations developed for vertical transverse isotropy at the expense of partly ignoring out-of-plane phenomena in multilayered azimuthally anisotropic HTI media.

NUMERICAL STUDY OF P -WAVE MOVEOUT IN HTI MEDIA

Here, we present results of a numerical study of P -wave reflection moveout in HTI media designed to test the accuracy of the hyperbolic and nonhyperbolic moveout equations introduced above. The exact traveltimes were computed using a 3-D anisotropic ray-tracing code developed by Gajewski and Pšenčík (1987). The moveout velocity on finite spreads was obtained by least-squares fitting of a hyperbolic moveout equation to the calculated traveltimes, i.e.,

$$V_{\text{mo}}^2 = \frac{\sum_{j=1}^N x_j^2}{\sum_{j=1}^N t_j^2 - N t_0^2}, \quad (16)$$

where x_j is the offset of the j -th trace, t_j is the corresponding two-way reflection traveltime, t_0 is the two-way vertical traveltime, and N is the number of traces.

Single HTI layer

Due to the presence of two orthogonal vertical symmetry planes in HTI media, it is sufficient to study reflection moveout in a single quadrant of azimuths (Figure 3). First, we test the accuracy of the P -wave hyperbolic moveout equation parameterized by the exact NMO velocity [equation (6)] on two models (Table 1), using two spreadlengths. Elastic coefficients for Model 1 are typical for a moderately anisotropic HTI medium caused by parallel vertical cracks (Thomsen, 1995), while Model 2 has much stronger azimuthal anisotropy that corresponds to higher values of the crack density.

As seen in Figure 4, the moveout velocity obtained from the exact traveltimes using equation (16) is generally close to the analytic NMO value [equation (6)] for conventional-length spreads ($X/D \leq 1$) (Figure 4a,c). (It should be mentioned that Model 2 is characterized by an uncommonly high magnitude of nonhyperbolic moveout.) Predictably, the difference between the two velocities increases on longer spreads (Figure 4b,d) due to the anisotropy-induced deviations of the moveout curve from a hyperbola.

Figure 4 also shows that the difference between the finite-spread and NMO velocity reaches its maximum in the symmetry-axis plane (azimuth $\alpha = 0^\circ$) and goes to zero in the isotropy plane ($\alpha = 90^\circ$). Clearly, despite the influence of out-of-plane phenomena (i.e., the deviation of the phase-velocity vector from the incidence plane), the magnitude of nonhyperbolic moveout outside the symmetry planes is *smaller* than in the direction of the symmetry axis. This result could be expected from the azimuthal dependence of the quartic moveout coefficient (10).

The inadequacy of the hyperbolic moveout equation (3) for long spreads is illustrated in more detail by Figure 5a,c showing the time residuals after the conventional hyperbolic moveout correction. Deviation of the hyperbolic curve from the exact traveltimes is much more pronounced for Model 2, which has an extremely large quartic

moveout term (Figure 5c). For such uncommonly strong nonhyperbolic moveout, conventional hyperbolic velocity analysis does not work well even on spreadlengths close to the reflector depth. In contrast, the nonhyperbolic moveout equation (5), which includes the exact quadratic and quartic moveout coefficients, provides excellent accuracy for both HTI models and for the whole range of offsets shown in Figure 5b,d. Application of the nonhyperbolic moveout equation reduces the residual moveout at large offsets (i.e., twice as large as the reflector depth) by a factor of ten compared with the residuals after the hyperbolic correction.

Multilayered HTI media

As discussed above, the conventional Dix equation is no longer strictly valid outside the symmetry planes of multilayered HTI media because the group-velocity vector does not lie in the incidence plane for the whole raypath. Still, for the three-layer HTI model (Model 3 from Table 2) in Figure 6, the effective normal-moveout velocity calculated by rms averaging of the exact interval values [equation (13)] is sufficiently close to the moveout velocity determined from hyperbolic moveout analysis on conventional-length spreads. A more detailed comparison between the generalized (exact) and conventional Dix equation in azimuthally anisotropic media is given in Tsvankin et al. (1997).

The maximum deviation of the NMO velocity from the finite-spread value is observed for the CMP line in the throughgoing symmetry-axis plane of the medium ($\alpha = 0^\circ$). As mentioned above, the Dix equation (13) is entirely valid for the NMO velocity in the symmetry-axis and isotropy planes. In both symmetry planes, the difference between the finite-spread and rms-averaged moveout velocity is caused entirely by the influence of nonhyperbolic moveout, which is much more pronounced in the symmetry-axis plane. In the isotropy plane, nonhyperbolic moveout is due to vertical velocity variation only; the effective gradient in the vertical velocity for

the model from Figure 6 is close to a typical value of 0.67 s^{-1} . The smaller magnitude of nonhyperbolic moveout away from the symmetry-axis plane makes the NMO equation (13) even more accurate in out-of-plane directions.

The difference between the exact traveltimes and the hyperbolic moveout equation (3) in Model 3 is displayed in Figure 7a. Clearly, the hyperbolic moveout equation based on the exact interval NMO velocities averaged by formula (13) provides a good approximation to the traveltimes on spreadlengths that do not exceed the reflector depth. This conclusion holds, albeit with a somewhat lower accuracy, even for Model 4 with layer-varying orientation of the symmetry axis (Figure 8a). We note, however, that the hyperbolic moveout equation breaks down if we disregard the azimuthal dependence of the interval NMO velocities described by equation (6). Application of any single value of NMO velocity would lead to misalignment of reflection events and poor stacking quality in certain ranges of azimuthal angles.

As in the homogeneous model, the error of the hyperbolic moveout equation increases with offset, this time due to the combined influence of anisotropy and layering (Figures 6–8). To describe long-spread moveout in layered HTI media, we use equation (5) with the effective values of the moveout coefficients given by equations (13), (14), and (15). Despite the approximate character of the averaging expressions, the nonhyperbolic moveout equation (5) provides high accuracy for both multilayered HTI media (Figures 7b and 8b). Similar to the result for single-layer models, the residual moveout at large offsets (twice the reflector depth) after the nonhyperbolic moveout correction is about one order of magnitude lower compared to the residual after the hyperbolic correction using equation (3).

In the previous examples, we examined reflection moveout in models consisting only of azimuthally anisotropic layers with the HTI symmetry. However, fractured reservoirs are often overlain by a nearly isotropic overburden, possibly with a vertical velocity gradient. Although it seems that the presence of isotropic layers should help to mitigate out-of-plane phenomena since phase- and group-velocity vectors in

isotropic media coincide with each other, deviation of the *group-velocity* vector from the incidence plane may even increase if we replace some of the HTI layers in the model by isotropic ones. Indeed, to keep the group-velocity vector close to the incidence plane, the character of azimuthal velocity variations should be similar throughout the section. In the limit of a single HTI layer (a completely uniform character of azimuthal anisotropy), the group-velocity vector is strictly confined to the incidence plane. During the transmission from an HTI layer into a purely isotropic medium, the phase-velocity vector stays in the same vertical plane, and the group-velocity vector has to coincide with the phase-velocity vector after the transmission. Since in the HTI layer the azimuths of the group- and phase-velocity vectors may be substantially different, this leads to an azimuthal rotation of the group vector at the boundary and potential errors in the averaging equations (13) and (14).

Nevertheless, as demonstrated by the example in Figure 10 for a model with five isotropic layers above a layer with HTI symmetry, our conclusions drawn for layered HTI models remain essentially valid in this case as well. The hyperbolic moveout equation parameterized by the NMO velocity (13) gives an adequate description of the moveout on conventional spreads, while the nonhyperbolic moveout equation (5) is close to the reflection traveltimes at large horizontal offsets. The improvement in accuracy gained by using the nonhyperbolic moveout equation is especially significant for the reflection from the bottom of the HTI layer. The accurate result for this (deepest) event was ensured by using the exact interval expressions (6) and (10) for the azimuthally dependent quadratic and quartic moveout coefficients. As before, the effective horizontal velocity for the reflection from the bottom of the HTI layer was obtained by fourth-power averaging [equation (15)]. However, for the purely isotropic overburden with a pronounced vertical-velocity gradient in Figure 10, equation (5) turns out to be somewhat more accurate with the effective V_{hor} equal to the maximum horizontal velocity of the medium above the reflector.

DISCUSSION AND CONCLUSIONS

We have presented an analytic description of nonhyperbolic (long-spread) reflection moveout in layered transversely isotropic media with horizontal symmetry axes. For a single-layer HTI model, the hyperbolic moveout equation parameterized by the exact NMO velocity given in Tsvankin (1997) provides a good approximation for P -wave traveltimes on conventional-length CMP spreads (close to the reflector depth). However, the accuracy of the hyperbolic equation rapidly decreases with offset due to the influence of anisotropy-induced nonhyperbolic moveout.

Our treatment of long-spread moveout is based on an exact expression for the azimuthally-dependent quartic moveout coefficient A_4 which has been derived for any pure mode in a homogeneous HTI layer with arbitrary strength of anisotropy. The expression for A_4 has an extremely simple form (7), with a single trigonometric function ($\cos^4 \alpha$, where α is the angle with the symmetry axis) multiplied with the quartic coefficient in the symmetry-axis plane. Therefore, the magnitude of nonhyperbolic moveout rapidly decreases with azimuth away from the symmetry-axis plane, where it can be obtained by analogy with VTI media. To account for deviations from hyperbolic moveout on long spreads (2-3 times as large as the reflector depth), we have substituted the exact azimuthally-dependent values of the NMO velocity and the quartic moveout coefficient into the nonhyperbolic moveout equation originally developed by Tsvankin and Thomsen (1994) for VTI media. Numerical examples show that this equation provides excellent accuracy for P -waves recorded in all azimuthal directions over an HTI layer, even for models with significant velocity anisotropy and pronounced nonhyperbolic moveout.

In multilayered HTI media, the moveout coefficients reflect the combined influence of layering, azimuthal and polar anisotropy. We show that the NMO velocity in a stack of horizontal HTI layers is given by the conventional rms averaging procedure if the *group-velocity* vector (ray) is confined to the incidence plane. Although the

rays in vertically inhomogeneous HTI media do diverge from the incidence plane on off-symmetry CMP lines, the magnitude of these deviations usually is not sufficient to cause measurable errors with use of the Dix equation, especially for models with a similar character of the azimuthal velocity variations in all layers (e.g., media with uniform orientation of cracks). Note that a more general Dix-type equation, that properly accounts for both azimuthal anisotropy and vertical inhomogeneity, was recently developed by Tsvankin et al. (1997).

To determine the quartic moveout coefficient A_4 in stratified HTI media, we use the same averaging equations as for vertical transverse isotropy (Hake et al., 1984; Tsvankin and Thomsen, 1994), but with the exact interval values of V_{nmo} and A_4 in each HTI layer. Then the NMO velocity and the quartic moveout coefficient, averaged over the stack of layers above the reflector, are used in the same nonhyperbolic moveout equation as in the single-layer model. Extensive numerical testing for stratified HTI media with both uniform and depth-varying orientation of the symmetry axis (as well as for models composed of HTI and isotropic layers) demonstrates sufficient accuracy of our nonhyperbolic approximation in the description of long-spread reflection moveout.

The nonhyperbolic moveout equation discussed here can serve as a replacement for ray tracing in modeling of long-spread reflection traveltimes in stratified media containing HTI, VTI and isotropic layers. It can also be used in the inversion of reflection data for horizontal transverse isotropy.

ACKNOWLEDGMENTS

We would like to thank Ken Larner and other members of the “Anisotropy Team” at the Center for Wave Phenomena (CWP) for useful discussions. We are also grateful to Tariq Alkhalifah (formerly CWP, now Stanford Exploration Project) for helpful suggestions and to Dirk Gajewski (University of Hamburg) for providing his 3-D

ray-tracing code. This work was partially supported by the Consortium Project on Seismic Inverse Methods for Complex Structures at CWP and by the United States Department of Energy (project "Velocity Analysis, Parameter Estimation, and Constraints on Lithology for Transversely Isotropic Sediments" within the framework of the Advanced Computational Technology Initiative). A. Al-Dajani would like to thank the Saudi Arabian Oil Company (Saudi Aramco) for the financial support; he is especially grateful to Mahmoud Abdul-Baqi of Saudi Aramco for making his scholarship possible.

REFERENCES

- Alkhalifah, T., 1997, Velocity analysis using nonhyperbolic moveout in transversely isotropic media: *Geophysics*, **62**, 1839-1854.
- Alkhalifah, T., and Tsvankin, I., 1995, Velocity analysis for transversely isotropic media: *Geophysics*, **60**, 1550-1566.
- Al-Chalabi, M., 1974, An analysis of stacking, rms, average, and interval velocities over a horizontally layered ground: *Geophysical Prospecting*, **22**, 458-475.
- Corrigan, D., Withers R., Darnall J., and Skopinski T., 1996, Fracture mapping from azimuthal velocity analysis using 3D surface seismic data: 66th Ann. Internat. Mtg., Soc. Expl. Geophys., Expanded Abstracts, 1834-1837.
- Crampin, S., 1985, Evidence for aligned cracks in the earth's crust: *First Break*, **3**, no. 3, 12-15.
- Dix, C. H., 1955, Seismic velocities from surface measurements: *Geophysics*, **20**, 68-86.

- Gajewski, D., and Pšenčík, I., 1987, Computation of high-frequency seismic wavefields in 3-D laterally inhomogeneous anisotropic media: *Geophys. J. R. Astr. Soc.*, **91**, 383-411.
- Gidlow, P.W., and Fatti, J.L., 1990, Preserving far offset seismic data using non-hyperbolic moveout correction: 60th Ann. Internat. Mtg., Soc. Expl. Geophys., Expanded Abstracts, 1726-1729.
- Grechka, V., and Tsvankin, I., 1996, 3-D description of normal moveout in anisotropic media: 66th Ann. Internat. Mtg., Soc. Expl. Geophys., Expanded Abstracts, 1487-1490.
- Hake, H., Helbig, K., and Mesdag, C. S., 1984, Three-term Taylor series for $t^2 - x^2$ curves over layered transversely isotropic ground: *Geophys. Prosp.*, **32**, 828-850.
- Hale, D., Hill, N.R., and Stefani, J., 1992, Imaging salt with turning seismic waves: *Geophysics*, **57**, 1453-1462.
- Hubral, P., and Krey, T., 1980, Interval velocities from seismic reflection time measurements: *Soc. Expl. Geophys.*
- Li, X.-Y., and Crampin, S., 1993, Approximations to shear-wave velocity and moveout equations in anisotropic media: *Geophys. Prosp.*, **41**, 833-858.
- Lynn, H., Simon, K., Bates, C., Van Doc, R., 1996, Azimuthal anisotropy in *P*-wave 3-D (multiazimuth) data: *The Leading Edge*, **15**, 923-928.
- Rüger, A., 1997, *P*-wave reflection coefficients for transversely isotropic models with vertical and horizontal axis of symmetry: *Geophysics*, **62**, 713-722.
- Sayers, C.M., and Ebrom, D.A., 1997, Seismic traveltime analysis for azimuthally anisotropic media: Theory and experiment: *Geophysics*, **62**, 1570-1582.

- Sena, A. G., 1991, Seismic travelttime equations for azimuthally anisotropic and isotropic media: Estimation of internal elastic properties: *Geophysics*, **56**, 2090-2101.
- Taner, M., and Koehler, F., 1969, Velocity spectra-digital computer derivation and application of velocity functions: *Geophysics*, **34**, 859-881.
- Thomsen, L., 1986, Weak elastic anisotropy: *Geophysics*, **51**, 1954-1966.
- Thomsen, L., 1988, Reflection seismology over azimuthally anisotropic media: *Geophysics*, **53**, 304-313.
- Thomsen, L., 1995, Elastic anisotropy due to aligned cracks in porous rock: *Geophysical Prospecting*, **43**, 805-830.
- Tsvankin, I., 1995, Normal moveout from dipping reflectors in anisotropic media: *Geophysics*, **60**, 268-284.
- Tsvankin, I., 1996, *P*-wave signatures and notation for transversely isotropic media: *Geophysics*, **61**, 467-483.
- Tsvankin, I., 1997, Reflection moveout and parameter estimation for horizontal transverse isotropy: *Geophysics*, **62**, 614-629.
- Tsvankin, I., Grechka, V., and Cohen, J.K., 1997, Normal-moveout velocity and generalized Dix equation for inhomogeneous anisotropic media: 67th Ann. Internat. Mtg., Soc. Expl. Geophys., Expanded Abstracts, 1246-1249.
- Tsvankin, I., and Thomsen, L., 1994, Nonhyperbolic reflection moveout in anisotropic media: *Geophysics*, **59**, 1290-1304.

TABLES

	Model 1	Model 2
$\epsilon^{(V)}$ (ϵ)	-0.143 (0.2)	-0.143 (0.2)
$\delta^{(V)}$ (δ)	-0.184 (0.1)	-0.318 (-0.2)
V_{Pvert} (V_{P0}) km/s	2.662 (2.25)	2.958 (2.5)
$V_{S^\perp vert}$ (V_{S0}) km/s	1.5 (1.5)	1.5 (1.5)

TABLE 1. Parameters of two single-layer HTI models used to generate the synthetic data in Figures 4 and 5. The layer thickness in both models is 1.5 km. $\epsilon^{(V)}$, $\delta^{(V)}$, V_{Pvert} , and $V_{S^\perp vert}$ are the HTI parameters of the equivalent VTI medium, while ϵ , δ , V_{P0} , and V_{S0} are the generic Thomsen parameters.

	Layer 1	Layer 2	Layer 3
$\epsilon^{(V)}$ (ϵ)	-0.143 (0.2)	-0.045 (0.05)	-0.143 (0.2)
$\delta^{(V)}$ (δ)	-0.184 (0.1)	-0.203 (-0.15)	-0.318 (-0.2)
$V_{P_{vert}}$ (V_{P0}) (km/s)	2.0 (1.69)	2.5 (2.384)	3.0 (2.535)
$V_{S^{\perp vert}}$ (V_{S0}) (km/s)	1.15 (1.15)	1.4 (1.4)	1.525 (1.525)
Depth of bottom (km)	0.5	1.0	1.5

TABLE 2. Parameters of the three-layer HTI model (Model 3) used to generate synthetic data in Figures 6 and 7. The axis of symmetry has the same orientation in all layers.

	Layer 1	Layer 2	Layer 3
$\epsilon^{(V)}$ (ϵ)	-0.143 (0.2)	-0.045 (0.05)	-0.143 (0.2)
$\delta^{(V)}$ (δ)	-0.184 (0.1)	-0.203 (-0.15)	-0.318 (-0.2)
$V_{P_{vert}}$ (V_{P0}) (km/s)	2.662 (2.25)	2.622 (2.5)	2.958 (2.5)
$V_{S^{\perp vert}}$ (V_{S0}) (km/s)	1.5 (1.5)	1.5 (1.5)	1.5 (1.5)
Depth of bottom (km)	0.7	1.0	1.5

TABLE 3. Parameters of the three-layer HTI model (Model 4) used to generate synthetic data in Figure 8. The symmetry axis in the first and third layer has the same direction, while in the second layer it is rotated by 60° .

APPENDIX A—QUARTIC MOVEOUT COEFFICIENT IN HTI MEDIA

Here, the approach suggested by Tsvankin (1997) in his derivation of the NMO velocity in HTI media is extended to obtain the quartic coefficient A_4 of the Taylor series expansion of the squared traveltime $[t^2(x^2)]$. First, we find an expression for A_4 in terms of the one-way traveltime from the zero-offset reflection point. Since a horizontal reflector coincides with a symmetry plane in HTI media, the group-velocity (ray) vector of any pure reflected wave in an HTI layer represents the mirror image of the incident ray with respect to the horizontal plane (Tsvankin, 1997; see Figures A-1 and A-2). This means that there is no reflection-point dispersal on CMP gathers above a homogeneous HTI layer, and we can represent the two-way traveltime along the specular raypath as the sum of the traveltimes from the zero-offset reflection point to the source and receiver (Figure A-1). The one-way traveltime from the reflection point to the source or receiver can be expanded in a Taylor series in the powers of the half-offset h , as suggested by Hale et al. (1992) in their derivation of the normal-moveout velocity from dipping reflectors. Here, we are interested in deriving the quartic moveout coefficient, so we will keep the quartic and lower-order terms in the Taylor series,

$$\begin{aligned} t(y+h) &= t(y) + h \frac{dt}{dx} + \frac{h^2}{2} \frac{d^2t}{dx^2} + \frac{h^3}{6} \frac{d^3t}{dx^3} + \frac{h^4}{24} \frac{d^4t}{dx^4} \dots; \\ t(y-h) &= t(y) - h \frac{dt}{dx} + \frac{h^2}{2} \frac{d^2t}{dx^2} - \frac{h^3}{6} \frac{d^3t}{dx^3} + \frac{h^4}{24} \frac{d^4t}{dx^4} \dots, \end{aligned} \quad (\text{A-1})$$

where all derivatives are evaluated at CMP location y .

Summing the two series expansions above, we obtain

$$t_h = t(y+h) + t(y-h) = t_0 + h^2 \frac{d^2t}{dx^2} + \frac{h^4}{12} \frac{d^4t}{dx^4}, \quad (\text{A-2})$$

where t_0 is the two-way zero-offset traveltime. Note that for a horizontal reflector beneath an HTI medium, both the phase- and group-velocity (ray) vectors of the zero-offset reflection are vertical.

Squaring both sides of equation (A-2) and ignoring terms of higher order than h^4 yields

$$t_h^2 = t_0^2 + \left[2t_0 \frac{d^2 t}{dx^2} \right] h^2 + \left[\left(\frac{d^2 t}{dx^2} \right)^2 + \frac{t_0}{6} \frac{d^4 t}{dx^4} \right] h^4. \quad (\text{A-3})$$

Comparing equation (A-3) with the Taylor's series expansion of the squared reflection traveltime $[t^2(x^2)]$

$$t_h^2 = t_0^2 + A_2(2h)^2 + A_4(2h)^4, \quad (\text{A-4})$$

we find the quadratic (A_2) and the quartic moveout coefficients (A_4) as

$$A_2 = \lim_{h \rightarrow 0} \left[\frac{t_0}{2} \frac{d^2 t}{dh^2} \right], \quad (\text{A-5})$$

and

$$A_4 = \frac{1}{16} \lim_{h \rightarrow 0} \left[\left(\frac{d^2 t}{dh^2} \right)^2 + \frac{t_0}{6} \frac{d^4 t}{dh^4} \right]. \quad (\text{A-6})$$

Tsvankin (1997) used equation (A-5) to derive the normal-moveout velocity ($V_{\text{nmo}}^2 = 1/A_2$) in a single HTI layer as a function of phase velocity and the symmetry-axis azimuth. Here, we apply equation (A-6) to obtain the quartic moveout coefficient A_4 . Equations (A-5) and (A-6) are valid for arbitrary anisotropic media if the specular reflection point does not change with offset within CMP gathers. It turns out, however, that reflection-point dispersal does not influence the value of normal-moveout velocity (or A_2) (Hubral and Krey, 1980, Appendix D; Tsvankin, 1995), and equation (A-5) can be used for both horizontal and dipping reflection events in media with any symmetry. Equation (A-6) for the quartic term is more restrictive and can be applied only in the absence of reflection-point dispersal (which is the case for our model).

We consider a CMP line that makes the azimuthal angle α with the symmetry axis (Figure A-2). Since the derivative dt/dh represents the apparent slowness within the CMP gather, it equals the projection of the slowness vector onto the CMP line,

$$p_h = \frac{dt}{dh},$$

and the quartic moveout coefficient [equation (A-6)] can be rewritten as

$$A_4 = \frac{1}{16} \lim_{h \rightarrow 0} \left[\left(\frac{dp_h}{dh} \right)^2 \right] + \frac{t_0}{96} \lim_{h \rightarrow 0} \left[\frac{d^3 p_h}{dh^3} \right] \quad (\text{A-7})$$

Introducing the group angle β in the incidence plane (Figure A-2) and taking into account that $h = z_0 \tan \beta$ and $z_0 = V_{vert} t_0/2$ (V_{vert} is the vertical velocity), we find

$$A_4 = \frac{1}{4t_0^2 V_{vert}^2} \lim_{\beta \rightarrow 0^\circ} \left[\left(\frac{dp_h}{d \tan \beta} \right)^2 \right] + \frac{1}{12t_0^2 V_{vert}^3} \lim_{\beta \rightarrow 0^\circ} \left[\frac{d^3 p_h}{d(\tan \beta)^3} \right]. \quad (\text{A-8})$$

It is convenient to represent β and p_h as functions of the phase angle θ with the symmetry axis (Figure A-2). Although the rays stay within the vertical incidence plane, the influence of azimuthal anisotropy moves the *phase-velocity* (slowness) vectors of the incident and reflected waves out of plane. Still, the phase-velocity vector in transversely isotropic media always lies in the plane formed by the symmetry axis and the group-velocity vector (Figure A-2). Rewriting the derivatives in equation (A-8) in terms of θ , we obtain

$$\frac{dp_h}{d \tan \beta} = \frac{dp_h}{d\theta} \frac{d\theta}{d \tan \beta}, \quad (\text{A-9})$$

and

$$\frac{d^3 p_h}{d(\tan \beta)^3} = \frac{d^3 p_h}{d\theta^3} \left(\frac{d\theta}{d \tan \beta} \right)^3 + 3 \frac{d^2 p_h}{d\theta^2} \frac{d^2 \theta}{d(\tan \beta)^2} \frac{d\theta}{d \tan \beta} + \frac{dp_h}{d\theta} \frac{d^3 \theta}{d(\tan \beta)^3}, \quad (\text{A-10})$$

where

$$\frac{d^2 \theta}{d(\tan \beta)^2} = \frac{d}{d \tan \beta} \left(\frac{d\theta}{d \tan \beta} \right) = \left[\frac{d}{d\theta} \left(\frac{d\theta}{d \tan \beta} \right) \right] \frac{d\theta}{d \tan \beta},$$

and similarly

$$\frac{d^3 \theta}{d(\tan \beta)^3} = \left[\frac{d}{d\theta} \left(\frac{d^2 \theta}{d(\tan \beta)^2} \right) \right] \frac{d\theta}{d \tan \beta}.$$

Substituting equations (A-9) and (A-10) into equation (A-8) yields

$$A_4 = \lim_{\theta \rightarrow 90^\circ} \left[\frac{1}{4t_0^2 V_{vert}^2} \left(\frac{dp_h}{d\theta} \frac{d\theta}{d \tan \beta} \right)^2 + \frac{1}{12t_0^2 V_{vert}^3} \frac{d^3 p_h}{d\theta^3} \left(\frac{d\theta}{d \tan \beta} \right)^3 \right] + \lim_{\theta \rightarrow 90^\circ} \left[\frac{1}{12t_0^2 V_{vert}^3} \frac{dp_h}{d\theta} \frac{d^3 \theta}{d(\tan \beta)^3} + \frac{1}{4t_0^2 V_{vert}^3} \frac{d^2 p_h}{d\theta^2} \frac{d^2 \theta}{d(\tan \beta)^2} \frac{d\theta}{d \tan \beta} \right]. \quad (\text{A-11})$$

Next, it is necessary to compute the derivatives in equation (A-11). From simple trigonometry (Figure A-2), we can relate the angle β to the group angle ψ of ray OR with respect to the symmetry axis as suggested in Tsvankin (1997):

$$\sin \beta = \frac{\cos \psi}{\cos \alpha},$$

and

$$\tan \beta = \frac{1}{\tan \psi \sqrt{1 - \frac{\sin^2 \alpha}{\sin^2 \psi}}}.$$

Then we express the group angle ψ through the phase angle θ and phase velocity $V(\theta)$ (Thomsen, 1986),

$$\tan \psi = \frac{\tan \theta + \frac{1}{V} \frac{dV}{d\theta}}{1 - \frac{\tan \theta}{V} \frac{dV}{d\theta}}. \quad (\text{A-12})$$

Applying the chain rule again, we have

$$\frac{d\theta}{d \tan \beta} = \frac{d\psi}{d \tan \beta} \frac{d\theta}{d\psi}.$$

Therefore,

$$\frac{d\theta}{d \tan \beta} = -\frac{\sin^2 \psi (1 - \frac{\sin^2 \alpha}{\sin^2 \psi})^{\frac{3}{2}}}{\cos^2 \alpha} \left[\frac{1 + (\frac{1}{V(\theta)} \frac{dV(\theta)}{d\theta})^2}{1 + \frac{1}{V(\theta)} \frac{d^2 V(\theta)}{d\theta^2}} \right]. \quad (\text{A-13})$$

By representing $\tan \beta$ as a function of ψ and θ , we are able to evaluate not only $\frac{d\theta}{d \tan \beta}$, but also the higher-order derivatives in equation (A-11) as well. Evaluating the derivatives at $\theta = \psi = 90^\circ$, we obtain

$$\left. \frac{d\theta}{d \tan \beta} \right|_{\theta=\psi=90^\circ} = -\cos \alpha \left[\frac{1}{1 + (\frac{1}{V} \frac{d^2 V}{d\theta^2})|_{\theta=90^\circ}} \right], \quad (\text{A-14})$$

and

$$\begin{aligned} \left. \frac{d^3 \theta}{d(\tan \beta)^3} \right|_{\theta=\psi=90^\circ} &= \left[\frac{\cos \alpha (2 + \sin^2 \alpha)}{1 + \frac{1}{V} \frac{d^2 V}{d\theta^2}} - \frac{\cos^3 \alpha (\frac{1}{V} \frac{d^2 V}{d\theta^2})^2 (3 + \frac{2}{V} \frac{d^2 V}{d\theta^2})}{(1 + \frac{1}{V} \frac{d^2 V}{d\theta^2})^4} \right]_{\theta=90^\circ} \\ &+ \left[\frac{\cos^3 \alpha \frac{1}{V} \frac{d^4 V}{d\theta^4}}{(1 + \frac{1}{V} \frac{d^2 V}{d\theta^2})^4} \right]_{\theta=90^\circ}. \end{aligned} \quad (\text{A-15})$$

The derivative $\frac{d\theta^2}{d(\tan \beta)^2} \Big|_{\theta=\psi=90^\circ}$ turns out to be unnecessary in equation (A-11) since $\frac{dp_h^2}{d\theta^2} \Big|_{\theta=\psi=90^\circ} = 0$.

To evaluate A_4 , we also need to find the derivatives of the projection of the slowness vector on the CMP line (p_h) with respect to the phase angle θ . Following Tsvankin (1997), we decompose the slowness vector (which is parallel to OD in Figure A-2) into two vectors parallel to sides OC and CD of triangle OCD. Then we find the horizontal projection of the slowness component parallel to CD using

$$\cos(\angle RCB) = \frac{\tan \beta \sin \alpha}{\sqrt{1 + \tan^2 \beta \sin^2 \alpha}} = \frac{\tan \alpha}{\tan \psi}.$$

Summing up the projections of both components onto the CMP line yields

$$p_h = \frac{1}{V} (\cos \theta \cos \alpha + \sin \theta \sin \alpha \tan \alpha / \tan \psi), \quad (\text{A-16})$$

with $\tan \psi$ determined by equation (A-12).

The derivatives of equation (A-16) with respect to θ , evaluated at $\theta = \psi = 90^\circ$, are given by

$$\frac{dp_h}{d\theta} \Big|_{\theta=\psi=90^\circ} = -\frac{1}{V_{vert} \cos \alpha} - \frac{1}{V_{vert} \cos \alpha} \left[\sin^2 \alpha \left(\frac{1}{V} \frac{d^2 V}{d\theta^2} \right) \Big|_{\theta=90^\circ} \right], \quad (\text{A-17})$$

$$\frac{dp_h^2}{d\theta^2} \Big|_{\theta=\psi=90^\circ} = 0, \quad (\text{A-18})$$

and

$$\frac{dp_h^3}{d\theta^3} \Big|_{\theta=\psi=90^\circ} = \frac{\cos \alpha}{V_{vert}} \left(1 + \frac{3}{V} \frac{d^2 V}{d\theta^2} \Big|_{\theta=90^\circ} \right) + \frac{\sin^2 \alpha}{V_{vert} \cos \alpha} \left(1 - \frac{1}{V} \frac{d^4 V}{d\theta^4} \Big|_{\theta=90^\circ} \right). \quad (\text{A-19})$$

Substitution of equations (A-14), (A-15), (A-17), (A-18), and (A-19) into equation (A-11) leads, after algebraic transformations, to a concise final result:

$$A_4 = \left[-\frac{\frac{4}{V} \frac{d^2 V}{d\theta^2} + 3 \left(\frac{1}{V} \frac{d^2 V}{d\theta^2} \right)^2 + \frac{1}{V} \frac{d^4 V}{d\theta^4}}{12t_0^2 V_{vert}^4 \left(1 + \frac{1}{V} \frac{d^2 V}{d\theta^2} \right)^4} \right]_{\theta=90^\circ} \cos^4 \alpha. \quad (\text{A-20})$$

Note that the first and third derivatives of the phase velocity in the vertical direction ($\theta = 90^\circ$) go to zero. Equation (A-20) is valid for any pure mode (P, S^\perp, S^\parallel) in HTI media with arbitrary strength of anisotropy.

**APPENDIX B—DIX EQUATION FOR LAYERED AZIMUTHALLY
ANISOTROPIC MEDIA**

In their derivation of the generalized Dix equation for anisotropic media, Alkhalifah and Tsvankin (1995) assumed that the phase and group-velocity vectors of incident and reflected waves are confined to the sagittal (incidence) plane. This implies that the incidence plane (i.e., the vertical plane that contains the CMP line) should be a symmetry plane of the medium, as well as the dip plane of the reflector. Here, we show that the generalized Dix equation retains the same form *outside* the symmetry planes of azimuthally anisotropic media, if the *group-velocity* vector does not deviate from the incidence plane for the whole ray path. Although this assumption cannot be satisfied exactly for multilayered azimuthally anisotropic models, it is helpful in gaining insight into the influence of azimuthal anisotropy on the accuracy of the Dix equation.

We consider CMP reflections from either a horizontal or a dipping interface overlain by a horizontally-layered arbitrary anisotropic medium (Figure B-1). Normal-moveout velocity in the CMP geometry can be represented as the the following function of the one-way traveltime t from the zero-offset reflection point [equation (A-5)]:

$$V_{\text{nmo}}^2 = \frac{2}{t_0} \lim_{h \rightarrow 0} \frac{d}{dh} \left(\frac{dt}{dh} \right)^{-1} = \frac{2}{t_0} \lim_{h \rightarrow 0} \frac{dh}{dp_h}, \quad (\text{B-1})$$

where h is half the source-receiver offset (h is positive in the down-dip direction), t_0 is the two-way zero-offset traveltime, and p_h is the projection of the slowness vector on the CMP line.

The ray parameter p (horizontal slowness), as well as p_h , remains constant along any ray above the reflector since the overburden is horizontally homogeneous. In the case considered by Alkhalifah and Tsvankin (1995), the slowness vector did not deviate from the incidence plane, and p_h was equal to p . However, as shown below, any difference between p_h and p has no influence on the form of the generalized Dix equation provided the group-velocity vector (ray) stays within the incidence plane.

Since we assume that the whole raypath is confined to the incidence plane, the half-offset h can be written as

$$h = \left(\sum_{i=1}^n x^{(i)} - x_0 \right),$$

where $x^{(i)}$ is the horizontal distance traveled by the ray in layer i (“horizontal displacement”), and x_0 is the total horizontal displacement of the zero-offset ray between the reflection point and the surface (Figure B-1). Substituting h into equation (B-1) yields

$$V_{\text{nmo}}^2 = \frac{2}{t_0} \lim_{h \rightarrow 0} \sum_{i=1}^n \frac{d(x^{(i)})}{dp_h}, \quad (\text{B-2})$$

To identify the interval values of NMO velocity in equation (B-2), let us draw an imaginary reflector through the intersection of the zero-offset ray with the bottom of layer i . The normal to the reflector is chosen to coincide with the slowness (phase) vector that corresponds to the segment of the zero-offset ray in this layer. Note that since the slowness vector associated with the zero-offset ray is allowed to be out of plane, the dip plane of the imaginary reflector is generally different from the incidence plane. Next, we imagine that the intersection of the zero-offset ray with the top of layer i represents a common-midpoint location of a gather parallel to the actual CMP line. Then the segment of the zero-offset ray in layer i will coincide with the raypath of the zero-offset CMP reflection from the imaginary interface. In accordance with equation (B-1), NMO velocity from the imaginary reflector at this CMP location will be given by

$$[V_{\text{nmo}}^{(i)}(\vec{s}^{(i)})]^2 = \frac{2}{t_0^{(i)}} \lim_{x^{(i)} \rightarrow x_0^{(i)}} \frac{d(x^{(i)})}{dp_h}, \quad (\text{B-3})$$

where $t_0^{(i)}$ is the two-way travelttime along the zero-offset ray in layer i , $x_0^{(i)}$ is the horizontal displacement of the zero-offset ray in layer i , and $\vec{s}^{(i)}$ is the slowness vector associated with the zero-offset ray. It follows that the summation in equation (B-2) is carried out over the NMO velocities from reflectors normal to the “zero-offset” slowness vectors in each layer. Substituting equation (B-3) into equation (B-2) yields

$$V_{\text{nmo}}^2 = \frac{1}{t_0} \sum_{i=1}^n t_0^{(i)} [V_{\text{nmo}}^{(i)}(\vec{s}^{(i)})]^2. \quad (\text{B-4})$$

Although this expression looks identical to the conventional Dix equation, interval NMO velocities in equation (B-4) correspond to reflectors with *different* dips determined by the orientation of the slowness vector associated with the zero-offset ray in each of the layers. In contrast with the symmetry-plane Dix equation obtained by Alkhalifah and Tsvankin (1995), equation (B-4) is influenced by the 3-D character of wave propagation since the normals to these reflectors (and the slowness vectors of the corresponding zero-offset rays) are not necessarily confined to the incidence plane (Figure B-1).

FIGURES

FIG. 1. Sketch of the transversely isotropic model with a horizontal symmetry axis caused by a system of parallel vertical cracks. HTI media contain two vertical planes of mirror symmetry defined by the crack orientation (after Rüger, 1997).

FIG. 2. Common-midpoint reflections on a line that makes the angle α with the symmetry plane of an HTI layer. Since the model has a horizontal symmetry plane, the incident and reflected rays of pure modes lie in the vertical incidence (sagittal) plane (after Tsvankin, 1997).

FIG. 3. Orientations of the survey lines over a horizontal HTI layer used in Figures 4 and 5.

FIG. 4. The influence of nonhyperbolic moveout on the estimation of P -wave normal-moveout velocity in a single HTI layer. The solid curve is the moveout velocity as a function of azimuth determined by fitting a hyperbola to the exact $t^2 - x^2$ curves [equation (16)]; the dashed curve is the normal-moveout (zero-spread) velocity from equation (6). The curves are calculated for two different HTI models (Table 1) and on two spreadlengths X : a) Model 1, $X/D = 1$ ($D = 1.5$ km is the reflector depth); b) Model 1, $X/D = 2$; c) Model 2, $X/D = 1$; d) Model 2, $X/D = 2$.

FIG. 5. Comparison between the exact traveltimes and moveout approximations in an HTI layer. The gray curves are the exact reflection traveltimes as functions of the offset-to-depth ratio for survey-line azimuths α of 0° , 30° , 45° , 60° , and 90° . (a) and (b) – Model 1 (Table 1); (c) and (d) – Model 2 (Table 1). The black curves in (a) and (c) are the time residuals after conventional hyperbolic moveout correction using equation (3), while the black curves in (b) and (d) are the residuals after the nonhyperbolic moveout correction using equation (5). The maximum error of both

approximations arises in the symmetry-axis plane (azimuth 0°), while in the isotropy plane (azimuth 90°) the reflection moveout is purely hyperbolic, and the error is zero.

FIG. 6. Accuracy of the Dix rms-averaging equation for P -wave normal-moveout velocity in layered HTI media. The solid curve is the moveout velocity as a function of azimuth determined by fitting a hyperbola to the exact t^2-x^2 curves [equation (16)] on two different spreadlengths: $X/D = 1$ (a), and $X/D = 2$ (b); the dashed curve is the normal-moveout (zero-spread) velocity from the Dix equation (13). The velocities are calculated for the reflection from the bottom of the third layer in a three-layer model with the same orientation of the symmetry axis in all layers (Model 3, Table 2). Note that the difference between the two velocities reaches its maximum in the symmetry-axis plane (azimuth 0°).

FIG. 7. Comparison between the exact traveltimes and the moveout approximations for a three-layer HTI model (Model 3 from Table 2 and Figure 6). The gray curves are the exact reflection traveltimes from all three interfaces for azimuths α of 0° , 30° , 45° , 60° , and 90° . The black curves in (a) are the time residuals after the conventional hyperbolic moveout correction using equation (3), with the NMO velocity from equation (13), while the black curves in (b) are the residuals after non-hyperbolic moveout correction using equation (5) with the effective coefficients from equations (13), (14), and (15).

FIG. 8. Comparison between the exact traveltimes and the moveout approximations for a three-layer HTI model with depth-varying orientation of the symmetry axis (Model 4, Table 3). The gray curves are the exact reflection traveltimes from all three interfaces for azimuths α of 0° , 30° , 45° , 60° , and 90° . The azimuthal angles are calculated with respect to the symmetry-axis direction in the first and third layer; the azimuth of the axis in the second layer is 60° . The black curves in (a) are

the time residuals after the conventional hyperbolic moveout correction using equation (3) with the NMO velocity from equation (13), while the black curves in (b) are the residuals after the nonhyperbolic moveout correction using equation (5) and the effective coefficients from equations (13), (14), and (15).

FIG. 9. Geometry of the synthetic experiment in Figure 10.

FIG. 10. Comparison between time residuals after moveout correction for a model that includes a stack of five homogeneous isotropic layers on top of an HTI layer (Figure 9). The curves in (a) are the time residuals for azimuths α of 0° , 30° , 45° , 60° , and 90° after the conventional hyperbolic moveout correction for all reflections using equation (3) with the NMO velocity from equation (13), while the curves in (b) are the residuals after the nonhyperbolic moveout correction using equation (5) and the effective V_{nmo} and A_4 from equations (13) and (14). The effective horizontal velocity for the isotropic layers is taken to be equal to the maximum horizontal velocity above the reflector; for the reflection from the bottom of the HTI layer, the horizontal velocity is calculated from equation (15). For layer 1 $V_P = 2.0$ km/s, and the depth $d_1=0.2$ km; for layer 2 $V_P = 2.5$ km/s, and $d_2=0.4$ km; for layer 3 $V_P = 3.0$ km/s, and $d_3=0.6$ km; for layer 4 $V_P = 3.5$ km/s, and $d_4=0.8$ km; for layer 5 $V_P = 2.5$ km/s, and $d_5=1.0$ km; for layer 6 the parameters are those for Model 2 (Table 1), $d_6=1.5$ km.

FIG. A-1. For a homogeneous HTI layer, the specular reflection point for any offset coincides with the zero-offset reflection point, and there is no reflection-point dispersal on CMP gathers. y denotes the CMP location and h is half the source-receiver offset.

FIG. A-2. The group- and phase-velocity vectors for the reflected waves in a ho-

mogeneous HTI layer. The incident (SO) and reflected (OR) group-velocity vectors (rays) lie in the vertical incidence plane and are symmetric with respect to the horizontal plane. The phase-velocity vector (direction OD) of the reflected ray OR is confined to the plane formed by OR and the axis of symmetry. Triangle RCB defines a plane normal to the symmetry axis (after Tsvankin, 1997).

FIG. B-1. Reflection from a dipping interface overlain by a sequence of horizontal, homogeneous, azimuthally anisotropic layers. We assume that the *rays* (group-velocity vectors) from the zero-offset reflection point are confined to the incidence plane but do not put any restrictions on the orientation of the corresponding *slowness* (phase-velocity) vectors. This implies that the normal to the reflector may deviate from the incidence plane.

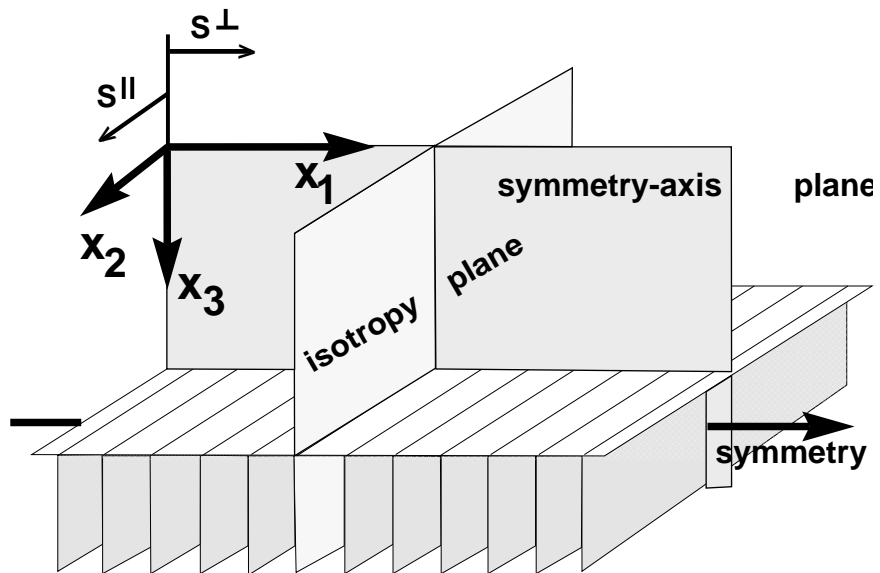


FIG. 1. Sketch of the transversely isotropic model with a horizontal symmetry axis caused by a system of parallel vertical cracks. HTI media contain two vertical planes of mirror symmetry defined by the crack orientation (after Rüger, 1997).

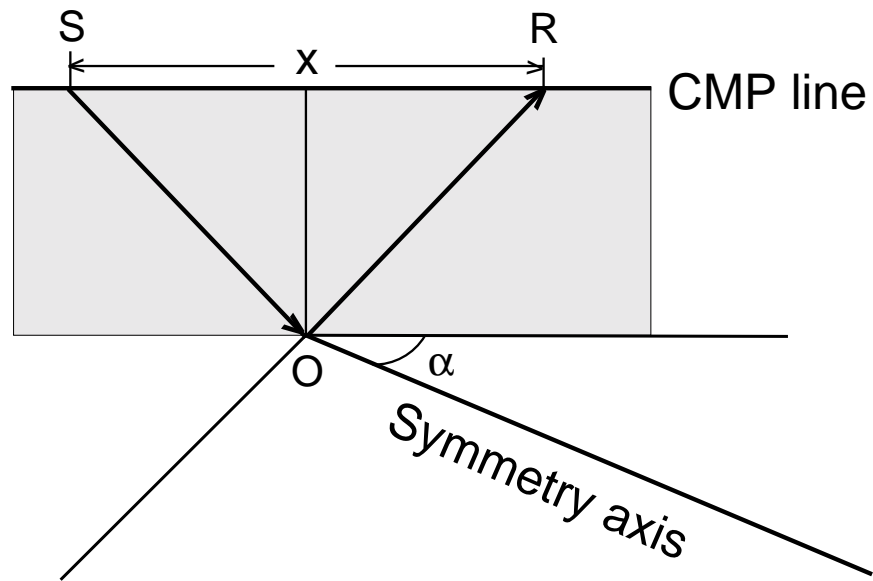


FIG. 2. Common-midpoint reflections on a line that makes the angle α with the symmetry plane of an HTI layer. Since the model has a horizontal symmetry plane, the incident and reflected rays of pure modes lie in the vertical incidence (sagittal) plane (after Tsvankin, 1997).

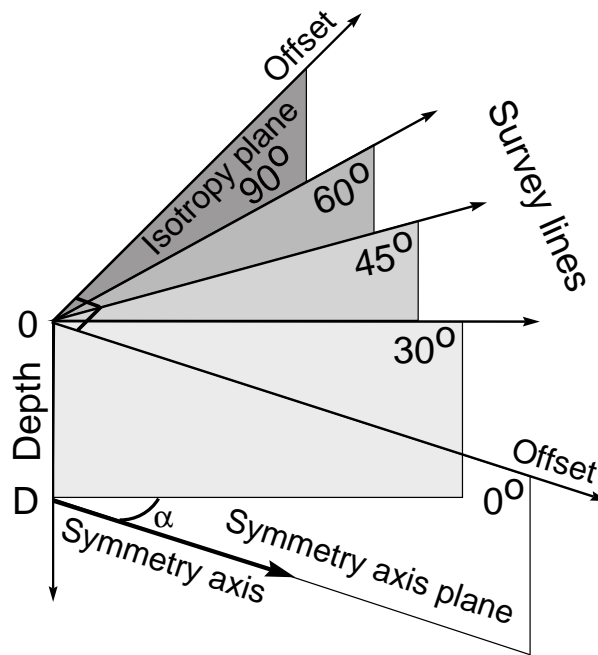


FIG. 3. Orientations of the survey lines over a horizontal HTI layer used in Figures 4 and 5.

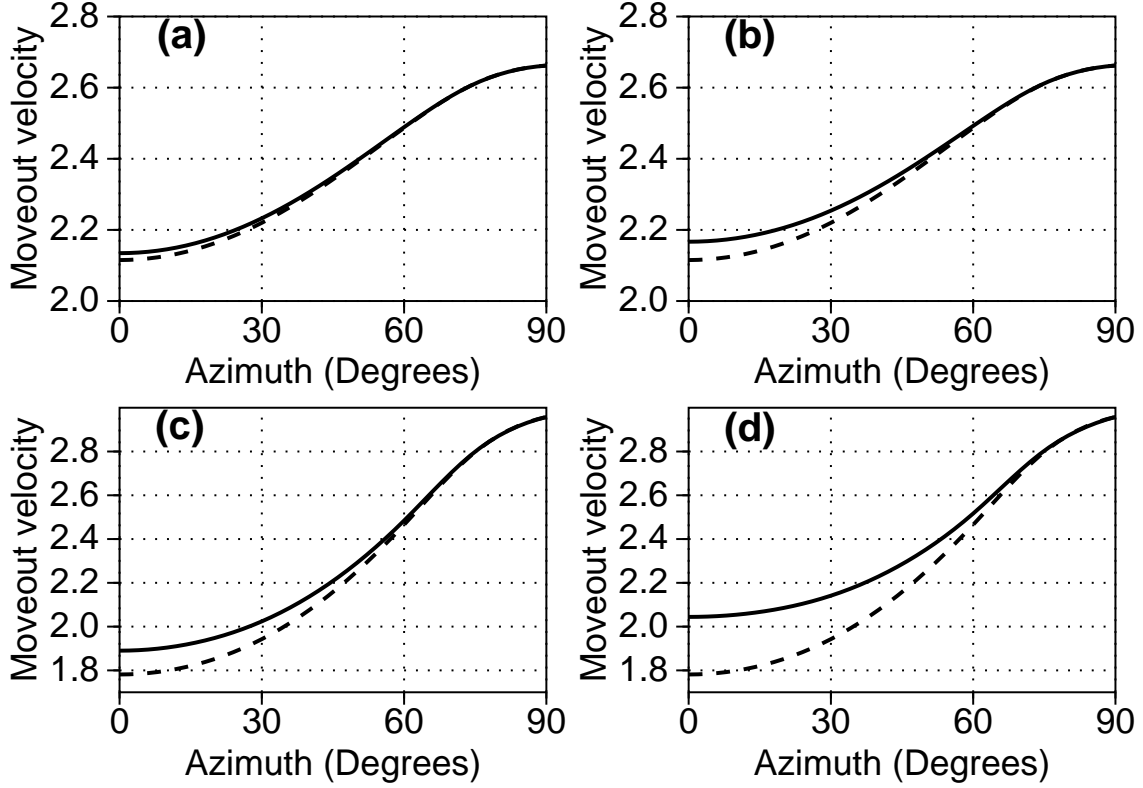


FIG. 4. The influence of nonhyperbolic moveout on the estimation of P -wave normal-moveout velocity in a single HTI layer. The solid curve is the moveout velocity as a function of azimuth determined by fitting a hyperbola to the exact $t^2 - x^2$ curves [equation (16)]; the dashed curve is the normal-moveout (zero-spread) velocity from equation (6). The curves are calculated for two different HTI models (Table 1) and on two spreadlengths X : a) Model 1, $X/D = 1$ ($D = 1.5$ km is the reflector depth); b) Model 1, $X/D = 2$; c) Model 2, $X/D = 1$; d) Model 2, $X/D = 2$.

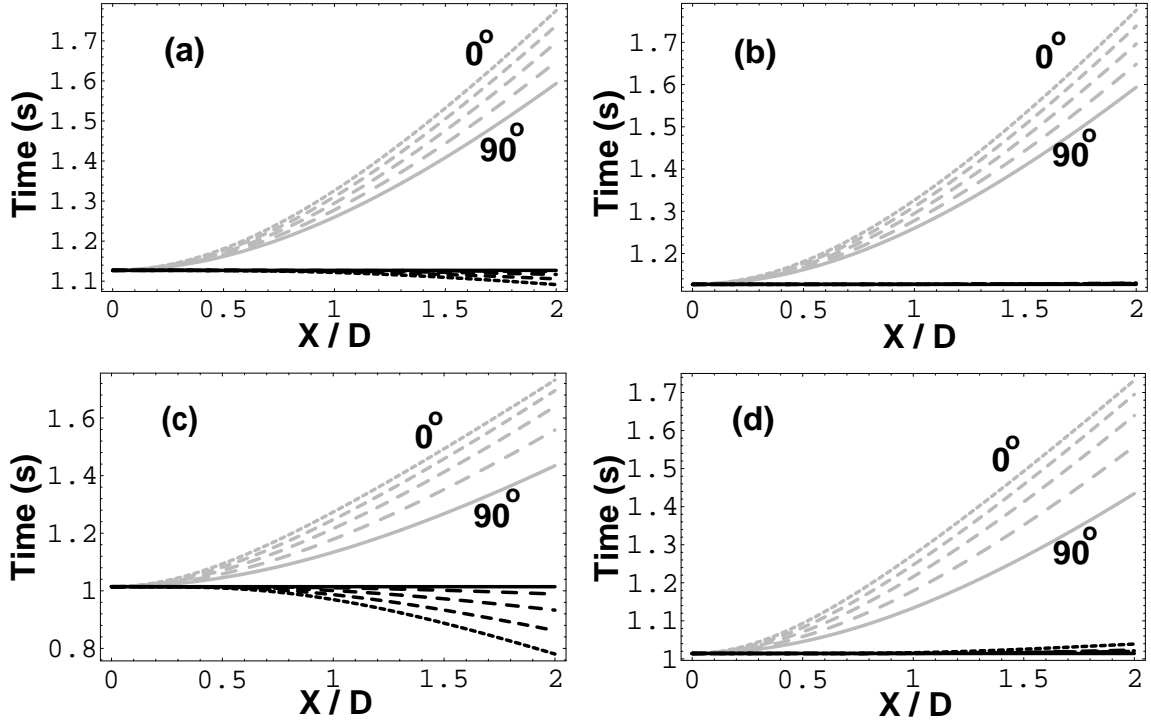


FIG. 5. Comparison between the exact traveltimes and moveout approximations in an HTI layer. The gray curves are the exact reflection traveltimes as functions of the offset-to-depth ratio for survey-line azimuths α of 0° , 30° , 45° , 60° , and 90° . (a) and (b) – Model 1 (Table 1); (c) and (d) – Model 2 (Table 1). The black curves in (a) and (c) are the time residuals after conventional hyperbolic moveout correction using equation (3), while the black curves in (b) and (d) are the residuals after the nonhyperbolic moveout correction using equation (5). The maximum error of both approximations arises in the symmetry-axis plane (azimuth 0°), while in the isotropy plane (azimuth 90°) the reflection moveout is purely hyperbolic, and the error is zero.

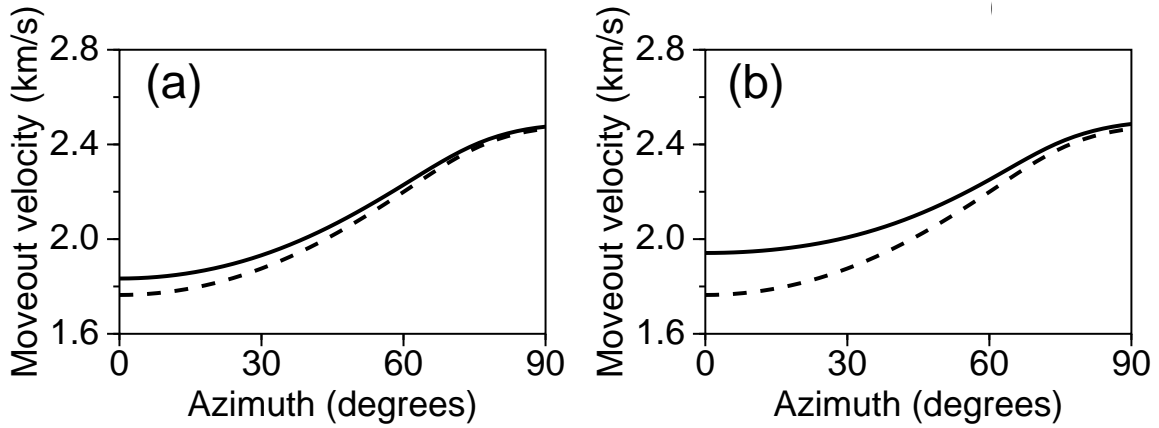


FIG. 6. Accuracy of the Dix rms-averaging equation for P -wave normal-moveout velocity in layered HTI media. The solid curve is the moveout velocity as a function of azimuth determined by fitting a hyperbola to the exact $t^2 - x^2$ curves [equation (16)] on two different spreadlengths: $X/D = 1$ (a), and $X/D = 2$ (b); the dashed curve is the normal-moveout (zero-spread) velocity from the Dix equation (13). The velocities are calculated for the reflection from the bottom of the third layer in a three-layer model with the same orientation of the symmetry axis in all layers (Model 3, Table 2). Note that the difference between the two velocities reaches its maximum in the symmetry-axis plane (azimuth 0°).

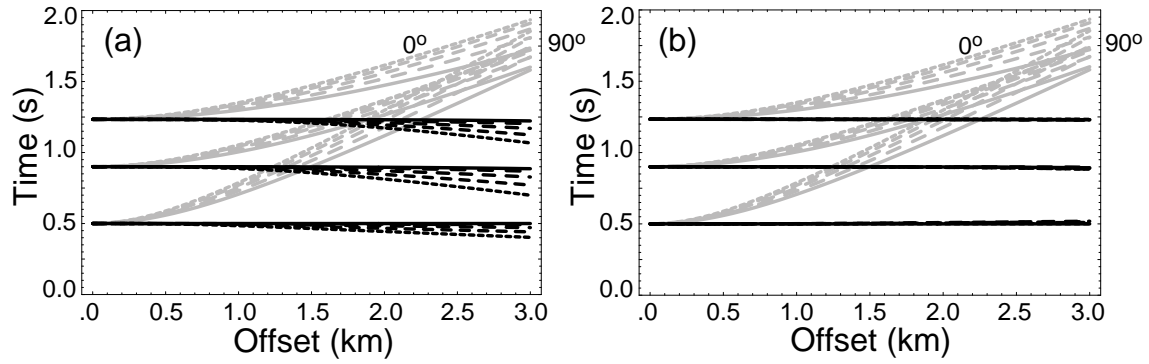


FIG. 7. Comparison between the exact traveltimes and the moveout approximations for a three-layer HTI model (Model 3 from Table 2 and Figure 6). The gray curves are the exact reflection traveltimes from all three interfaces for azimuths α of 0° , 30° , 45° , 60° , and 90° . The black curves in (a) are the time residuals after the conventional hyperbolic moveout correction using equation (3), with the NMO velocity from equation (13), while the black curves in (b) are the residuals after nonhyperbolic moveout correction using equation (5) with the effective coefficients from equations (13), (14), and (15).

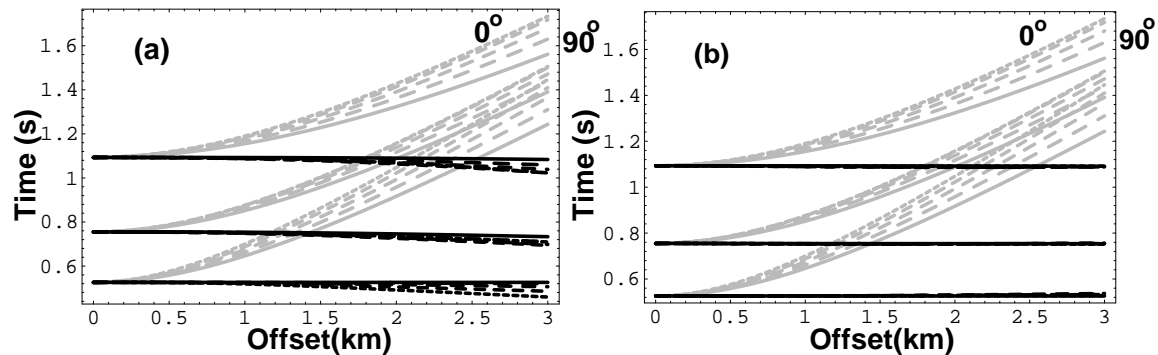


FIG. 8. Comparison between the exact traveltimes and the moveout approximations for a three-layer HTI model with depth-varying orientation of the symmetry axis (Model 4, Table 3). The gray curves are the exact reflection traveltimes from all three interfaces for azimuths α of 0° , 30° , 45° , 60° , and 90° . The azimuthal angles are calculated with respect to the symmetry-axis direction in the first and third layer; the azimuth of the axis in the second layer is 60° . The black curves in (a) are the time residuals after the conventional hyperbolic moveout correction using equation (3) with the NMO velocity from equation (13), while the black curves in (b) are the residuals after the nonhyperbolic moveout correction using equation (5) and the effective coefficients from equations (13), (14), and (15).

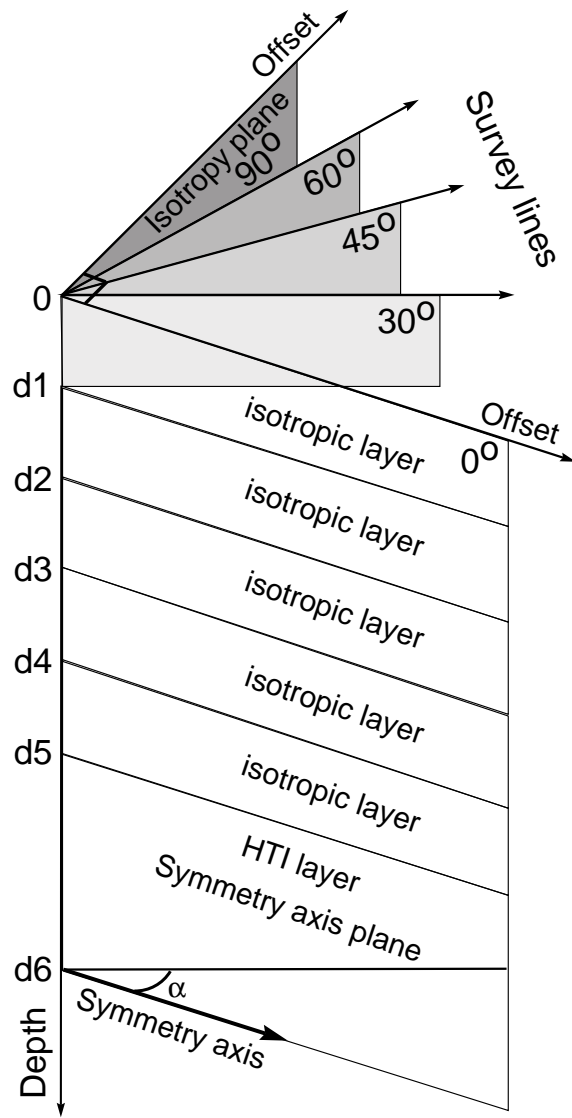


FIG. 9. Geometry of the synthetic experiment in Figure 10.

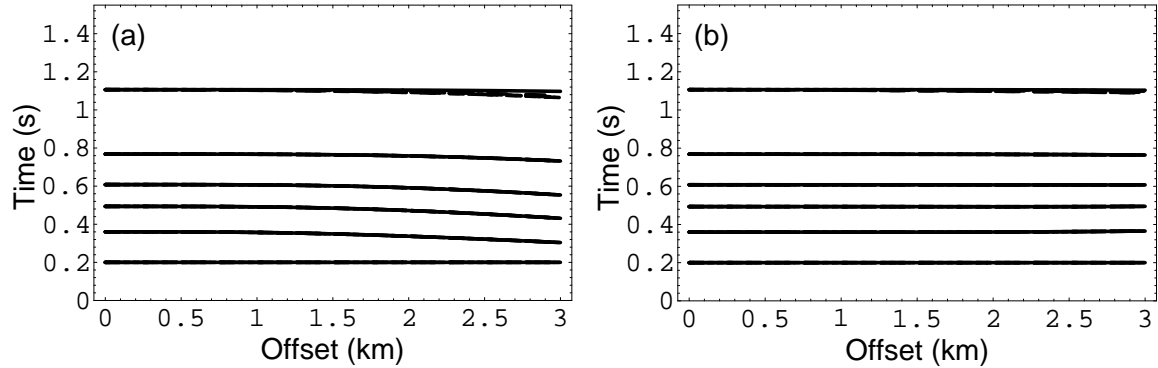


FIG. 10. Comparison between time residuals after moveout correction for a model that includes a stack of five homogeneous isotropic layers on top of an HTI layer (Figure 9). The curves in (a) are the time residuals for azimuths α of 0° , 30° , 45° , 60° , and 90° after the conventional hyperbolic moveout correction for all reflections using equation (3) with the NMO velocity from equation (13), while the curves in (b) are the residuals after the nonhyperbolic moveout correction using equation (5) and the effective V_{nmo} and A_4 from equations (13) and (14). The effective horizontal velocity for the isotropic layers is taken to be equal to the maximum horizontal velocity above the reflector; for the reflection from the bottom of the HTI layer, the horizontal velocity is calculated from equation (15). For layer 1 $V_P = 2.0$ km/s, and the depth $d_1=0.2$ km; for layer 2 $V_P = 2.5$ km/s, and $d_2=0.4$ km; for layer 3 $V_P = 3.0$ km/s, and $d_3=0.6$ km; for layer 4 $V_P = 3.5$ km/s, and $d_4=0.8$ km; for layer 5 $V_P = 2.5$ km/s, and $d_5=1.0$ km; for layer 6 the parameters are those for Model 2 (Table 1), $d_6=1.5$ km.

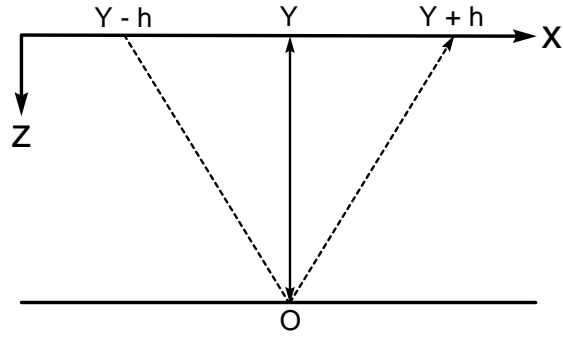


FIG. A-1. For a homogeneous HTI layer, the specular reflection point for any offset coincides with the zero-offset reflection point, and there is no reflection-point dispersal on CMP gathers. y denotes the CMP location and h is half the source-receiver offset.

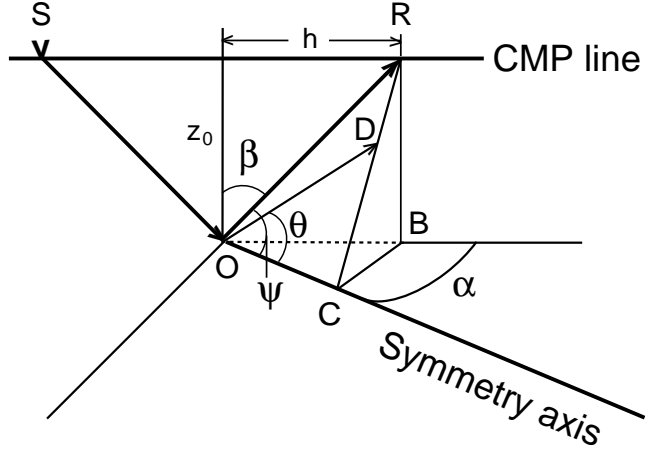


FIG. A-2. The group- and phase-velocity vectors for the reflected waves in a homogeneous HTI layer. The incident (SO) and reflected (OR) group-velocity vectors (rays) lie in the vertical incidence plane and are symmetric with respect to the horizontal plane. The phase-velocity vector (direction OD) of the reflected ray OR is confined to the plane formed by OR and the axis of symmetry. Triangle RCB defines a plane normal to the symmetry axis (after Tsvankin, 1997).

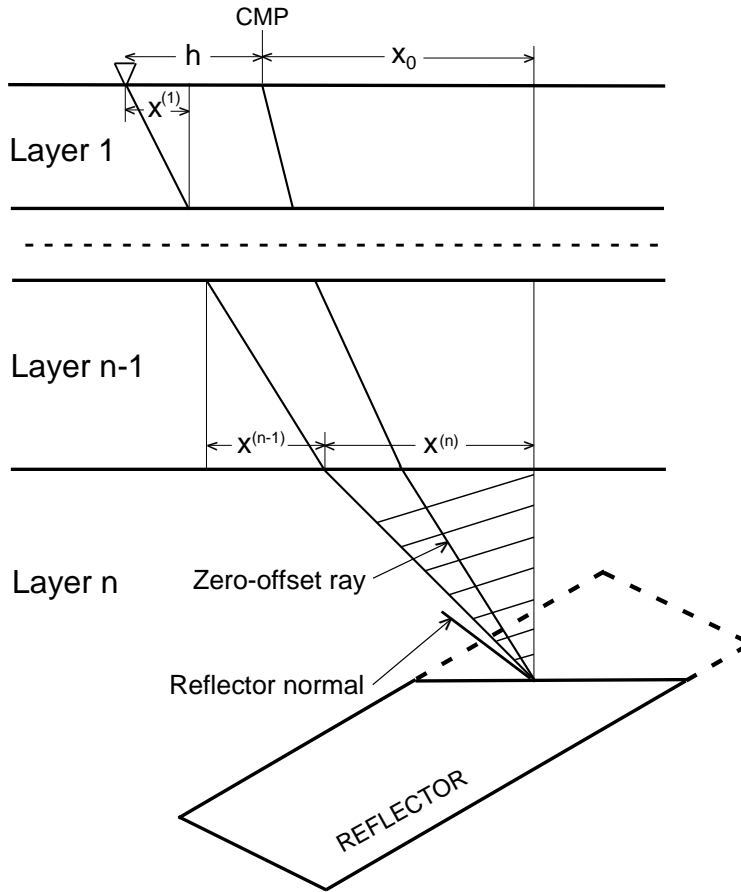


FIG. B-1. Reflection from a dipping interface overlain by a sequence of horizontal, homogeneous, azimuthally anisotropic layers. We assume that the *rays* (group-velocity vectors) from the zero-offset reflection point are confined to the incidence plane but do not put any restrictions on the orientation of the corresponding *slowness* (phase-velocity) vectors. This implies that the normal to the reflector may deviate from the incidence plane.